Original Article

CT features of hepatic epithelioid angiomyolipoma: differentiation from hepatocellular carcinoma in patients with noncirrhotic livers

Weihai Liu[1], Wenjie Liang[2]

[1]Department of Radiology, Beilun Branch Hospital of the First Affiliated Hospital, College of Medicine, Zhejiang University, the People's Hospital of Beilun District, Ningbo 315800, China; [2]Department of Radiology, the First Affiliated Hospital, College of Medicine, Zhejiang University, Hangzhou 310003, China

Correspondence to: Wenjie Liang, MD. Department of Radiology, the First Affiliated Hospital, College of Medicine, Zhejiang University, 79# Qingchun Road, Hangzhou 310003, China. Email: baduen@zju.edu.cn.

Background: Hepatic epithelioid angiomyolipoma (HEA) shares some similarities with other hepatic tumors, such as hepatocellular carcinoma (HCC). Thus, establishing a definite diagnosis of HEA based on medical imaging is often difficult. In this study, we evaluated multiphasic computed tomography (CT) imaging to differentiate HEA from HCC in patients with noncirrhotic livers.

Methods: We retrospectively analyzed the clinical and imaging data of both contrast and non-contrast enhanced CT scans from 25 patients with HEA and 50 patients with HCC in noncirrhotic livers. CT features, including lesion position, size, shape, interior content, border, enhancement degree, and enhancement pattern, were independently evaluated by two radiologists. Intratumoral blood vessels, peripheral supply vessels, the early display of the hepatic vein, peripheral abnormal perfusion, peripheral washout sign, pseudocapsule, and portal tumor thrombus were also evaluated. Next, we quantitatively analyzed difference within results of clinical and CT characteristics between the HEA and HCC groups.

Results: The number of female HEA patients is more than male (76% *vs.* 24%), with a mean age of 49.44±10.33 years (from 30 to 68 years). The majority (64%) of HEA patients were asymptomatic, without hepatitis (88%). On non-contrast enhanced CT, HEA mainly manifested as a round (92%), hypodense mass (100%) with little fat (12%) and rare complications, such as hemorrhage (4%) and calcification (4%). HEA all manifested as an intensely enhanced mass on contrast-enhanced CT. The differences between HEA and HCC were significant in the imaging characteristics of the early display of the hepatic vein (32% *vs.* 0%, P=0.000), intratumoral blood vessels during the nonarterial phase (36% *vs.* 8%, P=0.003), washout enhancement (52% *vs.* 86%, P=0.001), and prolonged enhancement (40% *vs.* 4%, P=0.000).

Conclusions: Although HEA is an uncommon hepatic tumor, clinical and CT manifestation may be indicative. Clinical and CT characteristics including asymptomatic, non-hepatic, fat-deficient, early display of the hepatic vein, intratumoral blood vessels during the nonarterial phase and prolonged enhancement are selected to improve the recognition of HEA, supporting for a differential diagnosis from HCC.

Keywords: Computed tomography; hepatic epithelioid angiomyolipoma; hepatocellular carcinoma (HCC); imaging

Submitted Apr 04, 2018. Accepted for publication Jul 11, 2018.
doi: 10.21037/qims.2018.07.01
View this article at: http://dx.doi.org/10.21037/qims.2018.07.01

Introduction

Hepatic angiomyolipoma, a benign tumor of mesenchymal origin, is a perivascular epithelioid cell tumor (PEComa) that was first reported by Ishak in 1976 (1). The epidemiology of hepatic angiomyolipoma remains unknown, but tuberous sclerosis accompanies approximately 13% of all cases.

However, many other cases are predominantly diffused (2). Hepatic angiomyolipoma comprises three components with different proportions, namely, abnormal blood vessels, fat cells, and smooth muscles. Concerning diagnostic imaging experiences in renal angiomyolipoma, hepatic angiomyolipoma could be diagnosed by preoperative computed tomography (CT) (3). Fatty and vascular components in tumors were later considered a characteristic manifestation of hepatic angiomyolipoma (2). However, the dependence of tumor heterogeneity on the proportions of different components sometimes complicates the preoperative diagnosis of hepatic angiomyolipoma, particularly when the fat content cannot be detected (4,5).

As a variant of hepatic angiomyolipoma, hepatic epithelioid angiomyolipoma (HEA) has obvious epithelioid cell components that differentiate it from classic angiomyolipoma (6,7). In the diagnosis of HEA, the exact proportions of epithelial components have not yet been determined. This epithelioid type of hepatic angiomyolipoma is also believed to have a low malignancy potential (8). Compared with kidney epithelioid angiomyolipoma, HEA is more commonly confirmed with a predominant composition of large epithelioid cells (9). Due to nuclear abnormalities, carcinoma-like morphology, and necrosis, HEA may be misdiagnosed by medical imaging or pathology (9). Thus, differentiating HEA and hepatocellular carcinoma (HCC) by immunohistochemistry (IHC) is necessary, especially for cases with alpha-fetoprotein (AFP) negative (9). Presently, the clinical characteristics, pathological histology, and IHC characteristics of HEA have been well documented (4,6-9). However, HEA imaging studies are rare (10-12). Because a thorough understanding of their imaging characteristics is lacking, up to 60% of HEA cases are preoperatively misdiagnosed as HCC (8), and HEA and HCC may require different therapeutic strategies. HCC can be treated by ablation, surgical resection or liver transplantation according to the clinical stage, whereas HEA necessitates resection alone because of its malignant potential.

Yang *et al.* (10) included 10 cases of HEA, which manifested as fat deficiency and hypervascularity on CT. Ji *et al.* (11) reported similar imaging characteristics of HEA, and the lack of a capsule was also considered a diagnostic clue. Recently, using contrast-enhanced CT, another study showed that HEA is similar to HCC (12). These imaging characteristics could be confusing in the imaging-based diagnosis of HEA and HCC on CT. To date, no reports have compared the imaging manifestations of HEA and HCC in response to this issue. To the best of our knowledge, this study reports the largest group of HEA cases. We aimed to provide a valuable catalog of CT imaging features for the preoperative diagnosis of HEA.

Methods

Inclusion criteria for study participants

This retrospective study was approved by the Ethics Committee of the First Affiliated Hospital, College of Medicine, Zhejiang University. We thoroughly searched the records of the pathological database of our institution from June 2009 to August 2016 with the keyword "hepatic epithelioid angiomyolipoma." The cases included in our study met the following criteria: (I) a pathological diagnosis of angiomyolipoma that could be categorized as epithelioid type; and (II) complete clinical and imaging data available for evaluation, including both unenhanced CT and contrast-enhanced CT scans. In total, 25 HEA cases were included in our study. Moreover, we randomly selected 50 noncirrhotic patients with a single HCC tumor who had undergone surgical resection in the same period. Reviewing the literatures and our own cases, I t shows nearly all of HEA occurred in noncirrhotic cases. Therefore, it may be clinically meaningful to compare HEA with HCC in noncirrhotic cases. According to the pathologic diagnostic criteria for cirrhosis, HCC in cirrhotic cases (Metavir F4 and decompensated cirrhosis) rather than hepatic fibrosis (Metavir F1-F3) cases were excluded. Then, complete clinical and CT imaging data from these 50 noncirrhotic HCC patients were collected for comparison with the HEA patients. The pathological specimens for all patients (both groups) were re-evaluated by two senior pathologists to obtain definitive results.

Clinical and imaging data and laboratory indices

The medical records of patients in this study were exported from the medical record management system. Patients' primary clinical symptoms, concomitant diseases and plasma AFP levels were then generalized and summarized. The inclusion indices included indices of hepatitis virus, concomitant diseases (fatty liver disease, cholelithiasis, hypertension, and diabetes), bad habits (smoking and alcohol abuse) and the plasma tumor marker (AFP).

CT scan protocol

A 16-row multidetector CT scanner (Aquilion 16, Toshiba

Medical Systems, Tokyo, Japan) was utilized to collect liver images. Seventy-five patients underwent a hepatic unenhanced CT scan and dynamic contrast-enhanced CT scan. The specific parameters of the hepatic CT scan were as follows: tube voltage, 125 kVp; tube current, 320 mA; spiral pitch, 0.95; reconstruction thickness, 2 mm; matrix, 510×510; and layer thickness, 2 mm. CT scan coverage ranged from the right diaphragmatic dome to the level of the inferior margin of the liver and spleen. A 1.5 mL/kg dose of a contrast agent, iohexol (Yangtze River Pharmaceutical Group, Taizhou, China), was injected as a bolus into the body through the elbow vein using a high-pressure injection pump at a rate of 3.0 mL/s. The hepatic dynamic contrast-enhanced CT scan had three-time phases, namely, the arterial (with the bolus-triggered technique, approximately 25–35 seconds), portal (60–70 seconds) and delayed (120–180 seconds) phases.

Classification of imaging findings

All CT imaging data from patients were acquired from the imaging report system of our institution and further evaluated in this study. None of the image readers were aware of the pathological results of patients from either group. Both radiologists (specializing in abdominal conditions) had more than ten years of experience in abdominal imaging diagnostics. The radiologists evaluated the CT images and summarized the final results, reaching an agreement through consultation. The evaluation of general CT characteristics included the lesion's position (left or right lobe), size (long-axis diameter), shape (round or irregular), internal density (hypodense or isodense; homogeneous or heterogeneous), inner composition (fat, hemorrhage, necrosis and calcification) and border (clear or ill-defined). In this study, adipose tissue was defined within the range of 20 to 80 HU.

During the arterial phase of the contrast-enhanced CT scan, we evaluated the imaging features, such as the enhancement degree of the lesion (intense or mild enhancement), consistency of enhancement (homogeneous or heterogeneous), intratumoral blood vessels, peripheral supplying vessels, the early display of the hepatic vein and peripheral abnormal perfusion. During the portal and delayed phase of the contrast-enhanced CT scan, we evaluated intratumoral blood vessels and peripheral washout signs, as well as pseudocapsules and portal thrombosis. The lesion enhancement pattern was evaluated simultaneously, including washout, prolonged enhancement, fade and poor blood supply. The 2014 version of the Liver Imaging Reporting and Data System (LI-RADS) was used to define the washout and fade (13). The pattern of prolonged enhancement was defined as a lesion presenting partial hyperdensity during each phase of the contrast-enhanced CT scan compared with hepatic tissues. The range of this enhancement might change over time. A poor blood supply was defined as a lesion that presented with hypo-enhancement during each phase of the contrast-enhanced scan compared with hepatic tissues.

Data analysis

Numerical variables, including patient age, lesion size, and plasma tumor marker (AFP) levels, are presented as the means plus standard deviations. Categorical variables, including clinical symptoms, concomitant diseases, the presence of hepatitis B infection, bad habits and AFP index, are presented as counts and percentages. SPSS 23.0 was used to perform statistical analyses. The numeration data were analyzed by the Chi-square test, and the measurement data were first grouped for a normal distribution. If each group had a normal distribution, the count data were analyzed by independent samples *t*-test using the "mean ± standard deviation." If the groups had a non-normal distribution, then measurement data were analyzed by a nonparametric test using the median (25–75% digit), including the following: comparison of clinical features, comparison of general imaging features, and comparison of CT enhancement patterns.

Results

Clinical data and laboratory indices

Eventually, 25 HEA definitively diagnosed by the pathology of surgically excised (21 cases) or biopsy (4 cases) specimens were included in this study. And 50 noncirrhotic HCC cases were confirmed by surgical resection also included in the study. However, 11 HEA case were excluded in our study because of the lack of CT data.

The age of HEA patients ranged from 30 to 68, with an average of 49.44±10.33 years. HEA occurrence proportion of female and male was approximate 4:1. Intrahepatic lesions were observed during health examinations or clinical screenings in 16 patients; among these patients, 9 exhibited clinical symptoms for relatively large diameter lesions. There were 5 cases of abdominal pain, 2 cases of

Table 1 Clinical features and comparison between HEA and HCC in noncirrhotic livers

Features	HEA (n=25)	HCC (n=50)	χ^2	P
Gender			20.25	0.000*
Male	6 (24%)	39 (78%)		
Female	19 (76%)	11 (22%)		
Age	49.44±10.33	56.50±11.84	–2.504	0.015*
Symptoms			0.804	0.370
Asymptomatic	16 (64%)	37 (74%)		
Symptomatic	9 (36%)	13 (26%)		
Hepatitis B	3 (12%)	41 (82%)	33.679	0.000*
Fatty liver disease	0 (0%)	3 (6%)	1.563	0.211
Cholelithiasis	1 (4%)	4 (8%)	0.429	0.513
Hypertension	3 (12%)	16 (32%)	3.524	0.060
Diabetes	0 (0%)	8 (16%)	4.478	0.034*
Smoking	2 (8%)	16 (32%)	5.263	0.022*
Alcohol abuse	4 (16%)	16 (32%)	2.182	0.14
Elevated AFP	0 (0%)	22 (44%)	15.566	0.000*

*, P<0.05 indicates a significant difference between the two groups. HEA, hepatic epithelioid angiomyolipoma; HCC, hepatocellular carcinoma; AFP, alpha-fetoprotein.

abdominal distension, 1 case of abdominal distress and 1 case of feebleness and poor appetite. The age of HCC patients ranged from 33 to 80, with an average of 56.50±11.84 years. Thirty-seven patients did not exhibit any symptoms, and 19 patients exhibited clinical symptoms. There were 12 cases of abdominal pain, 4 cases of abdominal distension, 2 cases of abdominal distress and 1 case of feebleness and poor appetite.

There were 22 cases of elevated plasma AFP among patients in the HCC group [22.6–15,345.2 U/mL, average 2,356.43±4,435.43 U/mL (reference value, 0–20 U/mL)]. Clinical data and summarized comparisons are presented in *Table 1*.

Differences in gender, age, hepatitis virus infection, diabetes, smoking and AFP levels between patients in the HEA group and those in the HCC group were significant. *Table 1* shows clinical features and summarized comparisons between both groups.

CT imaging findings and comparison

The lesion diameter in the 25 HEA cases ranged from 1.5 to 7.8 cm (average 3.76±1.71 cm). The diameters in the 50 HCC cases ranged from 1.5 to 11.2 cm (average 4.00±2.32 cm). The general CT features and comparisons of both groups are summarized in *Table 2*. Statistical analyses confirmed a significant difference in the inner necrosis of lesions between the HEA and HCC groups (0% *vs.* 24%, P=0.008).

The comparison of enhancement patterns between both groups is summarized in *Table 3*. We detected significant differences in the early display of the hepatic vein during the arterial phase (32% *vs.* 0%, P=0.000), intratumoral blood vessels during the portal/delayed phase (36% *vs.* 8%, P=0.003), washout enhancement pattern (52% *vs.* 86%, P=0.001) and prolonged enhancements (40% *vs.* 4%, P=0.000) between the HEA and HCC groups (*Figures 1-5*). The differences in other imaging features were nonsignificant.

Histopathological findings

Pathologically, among 25 cases of HEA, epithelioid cells were usually mixed with a small amount of mature fat tissues. The fat composition of the 23 HEAs was less than 10%, 5 of which were without definite fatty cells. And the fat composition of 2 HEAs was 10–20% and

Table 2 General CT features and comparison between HEA and HCC in noncirrhotic livers

Features	HEA (n=25)	HCC (n=50)	χ^2	P
Position			0	1.000
Left lobe	7 (28%)	14 (28%)		
Right lobe	18 (72%)	36 (72%)		
Long-axis diameter	3.76±1.71	4.00±2.32	–0.467	0.642
Shape			0.528	0.467
Round	23 (92%)	48 (96%)		
Irregular	2 (8%)	2 (4%)		
Internal density			0.507	0.447
Hypodense	25 (100%)	49 (98%)		
Isodense	0 (0%)	1 (2%)		
Density consistency			0.667	0.414
Homogeneous	14 (56%)	23 (46%)		
Heterogeneous	11 (44%)	27 (54%)		
Fat	3 (12%)	2 (4%)	1.714	0.190
Hemorrhage	1 (4%)	1 (2%)	0.257	0.612
Necrosis	0 (0%)	12 (24%)	7.143	0.008*
Calcification	1 (4%)	0 (0%)	2.027	0.155
Border			2.827	0.093
Clear	24 (96%)	41 (82%)		
Ill-defined	1 (4%)	9 (18%)		

*, P<0.05 indicates a significant difference between the two groups. HEA, hepatic epithelioid angiomyolipoma; HCC, hepatocellular carcinoma.

30–40%. Among 50 cases of HCC, 34 cases were highly differentiated HCC, 12 cases were moderately differentiated HCC, and 4 cases were poorly differentiated HCC. In the 71 resected cases, liver tissues around the tumor in the resected specimen were confirmed as noncirrhotic hepatic parenchyma.

Discussion

Notably, in our study, HEA was more likely to occur in females than in males. The incidence of HCC in males in this study was approximately three times as high as that in females, which was similar to previous reports regarding the incidence rate of HCC in populations in this area (14). This result reflected the difference in the sex distribution between HEA and HCC. Consistent with the previously reported incidence rate of hepatitis virus infection among the general population in this area, only 12.0% of patients had hepatitis virus infection in the HEA group (15). Moreover, as a result of hepatitis virus infection, the proportions of diabetes and smoking in the HCC group were higher than those in the HEA group (16,17). Additionally, the detection of plasma AFP contributed to the differentiation of HEA from HCC in noncirrhotic livers. Furthermore, none of the cases of HEA in our study were accompanied by tuberous sclerosis, which was consistent with previous reports that hepatical AML was rarely associated with TSC in China (8). So, the molecular mechanism of HEA needs further investigation. It was also worth mentioning that the proportion of HCC differentiation in our study is acceptable, which was dominated by high and moderate differentiation. Therefore, the comparison between the two groups may help us to get

Table 3 Contrast-enhanced CT features and comparison between HEA and HCC in noncirrhotic livers

Features	HEA (n=25)	HCC (n=50)	χ^2	P
Arterial phase				
Intense enhancement	25 (100%)	49 (98%)	0.507	0.477
Homogeneous	2 (8%)	5 (10.2%)	0.094	0.759
Heterogeneous	23 (92%)	44 (89.8%)		
Mild enhancement	0 (0%)	1 (2%)	0.507	0.477
Intratumoral blood vessels	11 (44%)	20 (40%)	0.11	0.740
Peripheral supplying vessels	22 (88%)	35 (70%)	2.961	0.085
Early display of the hepatic vein	8 (32%)	0 (0%)	17.91	0.000*
Peripheral abnormal perfusion	3 (12%)	3 (6%)	0.815	0.367
Portal and delayed phase				
Intratumoral blood vessels	9 (36%)	4 (8%)	9.119	0.003*
Peripheral washout signs	0 (0%)	3 (6%)	1.563	0.211
Pseudocapsule	3 (12%)	6 (12%)	0	1.000
Portal vein thrombosis	0 (0%)	2 (4%)	1.027	0.311
Enhancement pattern				
Washout	13 (52%)	43 (86%)	10.186	0.001*
Prolonged enhancement	10 (40%)	2 (4%)	16.071	0.000*
Fade	2 (8%)	4 (8%)	0	1.000
Poor blood supply	0 (0%)	1 (2%)	0.507	0.477

*, P<0.05 indicates a significant difference between the two groups. HEA, hepatic epithelioid angiomyolipoma; HCC, hepatocellular carcinoma.

valuable diagnostic features.

The detection of intratumoral fat composition is of great significance in narrowing the range of differential diagnoses in hepatic lesions. Intratumoral fat is considered as a valuable diagnostic clue for HEA (3,18). Because of the deficiency of fat cell or the scattered distribution of a few fat cells in the tumor, preoperative fat detection is a limited imaging diagnostic clue for HEA. In our study, only 3 patients (12%) in the HEA group exhibited fatty compositions on CT. Similarly, through a review of MRI manifestations of 22 HEA cases, the fatty composition detected in 9 HEA cases was lower than that in 13 non-HEA cases (19). Furthermore, more than half of HEA cases did not exhibit a fatty composition on MRI (19). We speculate that the different results and different proportions of fat in the tumor are due to the reduced fat composition and different instruments used in detection. Although the efficacy of CT in detecting fatty composition is inferior to that of MRI, the low detection of intratumoral fat reflects the pathological characteristic of the lower fat composition of HEA. Moreover, the difference in the detection of intratumoral fat between HEA and HCC patients was nonsignificant. Therefore, considering the possibility of HEA when encountering a fatless liver tumor in the clinic is necessary. The detection of fat by CT is restricted, and several studies have confirmed that MRI has an advantage in evaluating fat composition (20,21). Studies have validated certain MRI characteristics (e.g., an early draining vein, intratumoral blood vessels, lack of pseudocapsules, and high ADC values) as contributors to the identification of hepatic angiomyolipoma and fat-containing HCC (19). We suggest that these features might also be helpful in the differential diagnosis of HEA from fat-containing HCC in CT. In the case of clinically suspected HEA, MRI examination might be performed to increase the imaging information for judgment.

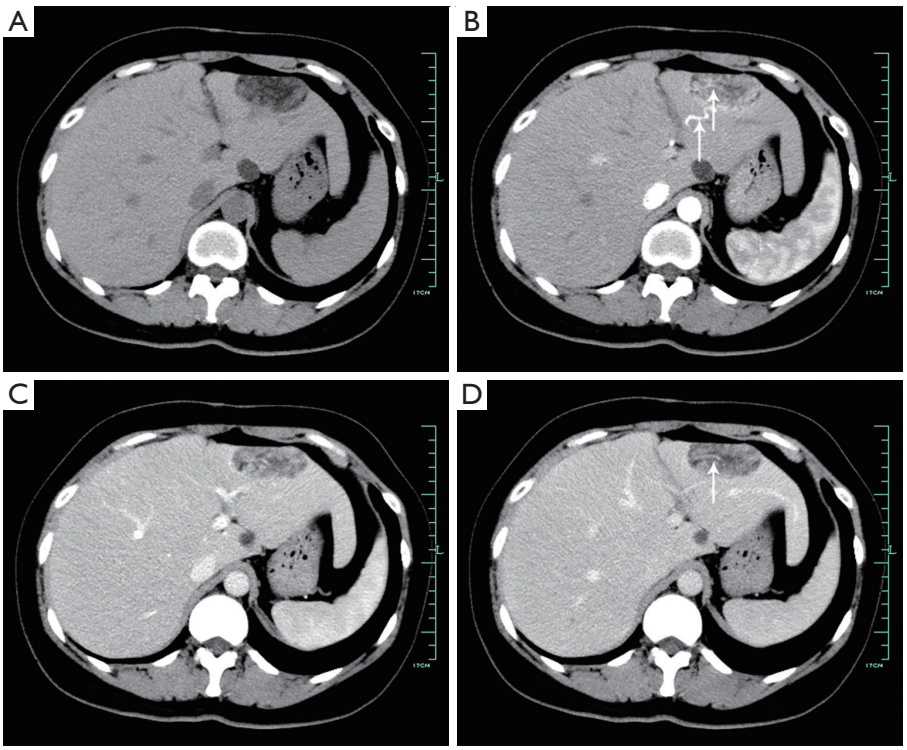

Figure 1 A 37-year-old female with an asymptomatic hepatic mass. (A) A plain CT scan shows a circumscribed mass with a size of 2.4 cm × 5.3 cm in the left lobe containing large amounts of fat components. (B) During the arterial phase, the mass shows heterogeneous enhancement with a supplying blood vessel and intratumoral blood vessel (arrows). (C,D) Enhancement of the mass is slightly decreased during the portal phase and delayed phase, with an intratumoral blood vessel (arrow).

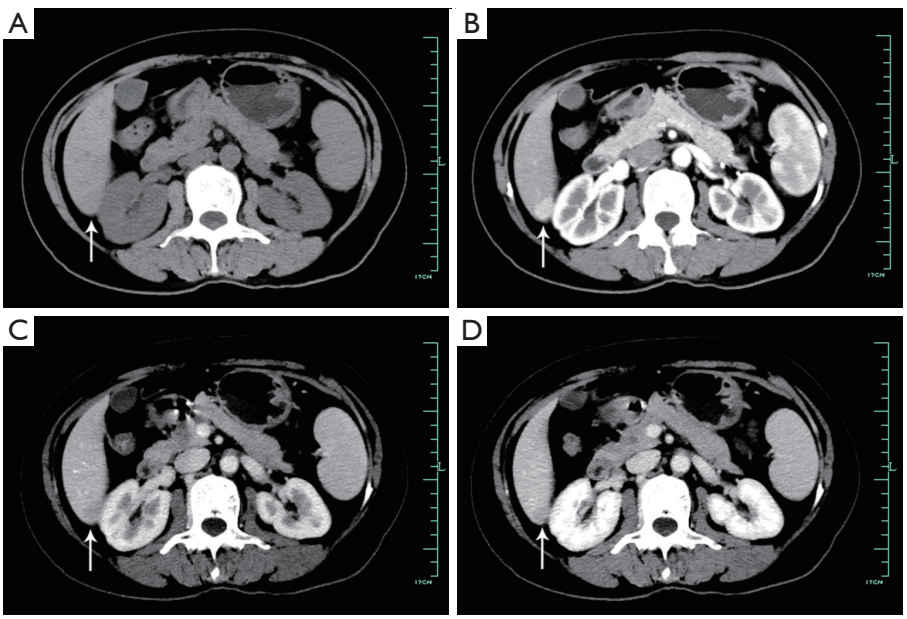

Figure 2 A 57-year-old female with an accidental hepatic nodule (arrow). (A) A plain CT scan shows an ill-defined nodule in the right lobe. (B) The nodule shows marked enhancement during the arterial phase. (C,D) The mass washed out during the portal phase and delayed phase.

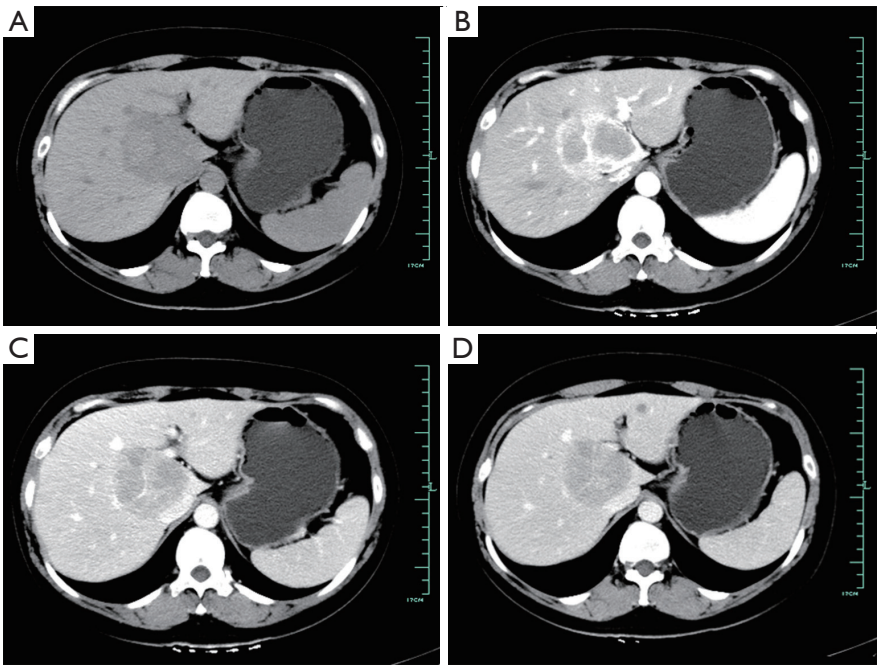

Figure 3 A 34-year-old female with left upper abdominal pain. (A) A plain CT scan shows a heterogeneous hypodense hepatic mass adjacent to the second hepatic hilum. (B) An arterial phase image shows peripheral enhancement and septal enhancement of the mass. (C,D) Portal phase and delayed phase images show an enhancing hypoattenuating mass with septal enhancement.

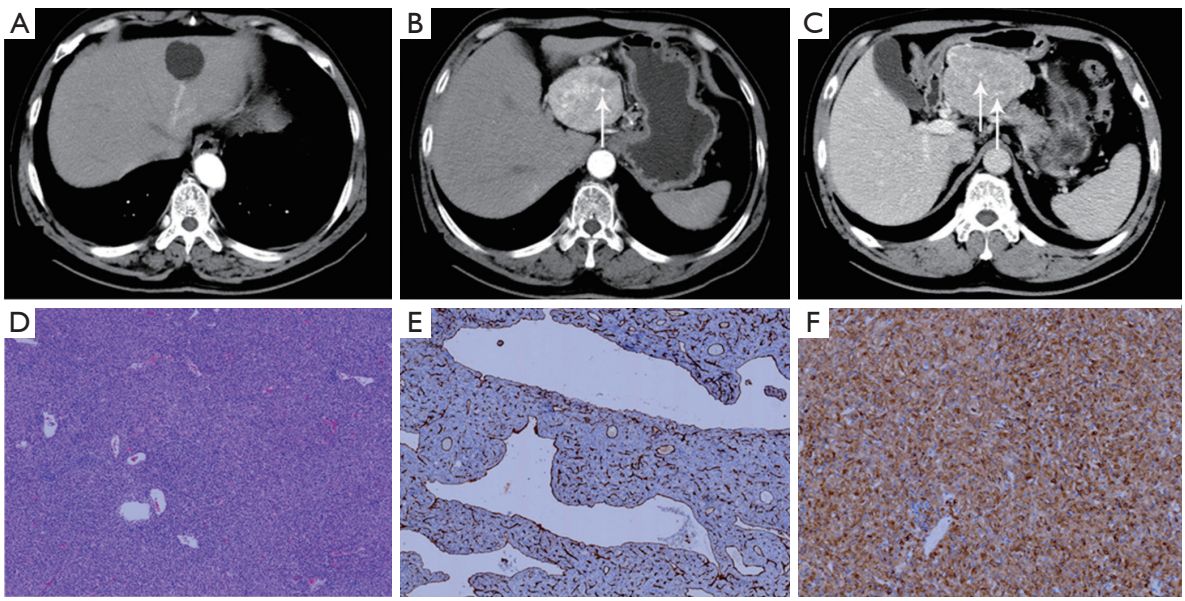

Figure 4 A 63-year-old male with feebleness and poor appetite. (A) An axial contrast-enhanced CT image shows that the early display of the left hepatic vein is evident during the arterial phase. (B) Heterogeneous enhancement of the mass during the arterial phase where vascularity is visible inside the mass (arrow). (C) During the portal phase, the mass presented with relative hypo-enhancement, and vascularity is visible inside the lesion (arrows). (D) Pathologic microscopy shows that the tumor is composed of a small amount of fat cells and numerous hypochromatic cells with a slightly eosinophilic cytoplasm (×40, HE stain) and deformed vessels (E, ×100; CD34 stain). (F) The IHC finding is positive for HMB45 (×200).

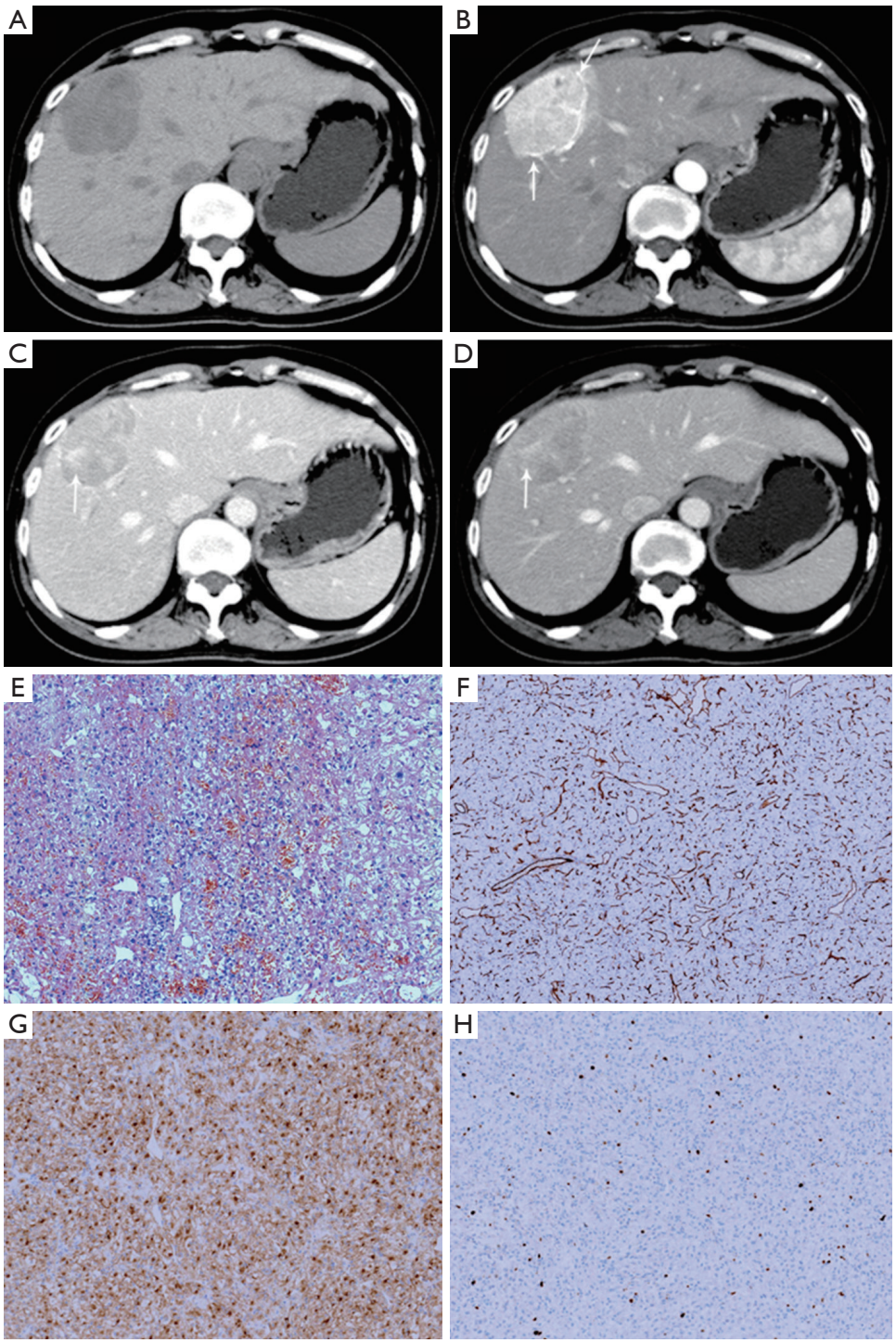

Figure 5 A 53-year-old female with upper abdominal distention. (A) A mildly heterogeneous hypodense mass is revealed via unenhanced CT scan. (B) An intense heterogeneously enhanced mass is revealed during the arterial phase. Tortuous vessels are visible both around and inside the lesion (arrow). (C,D) During the portal phase and delayed phase, some areas continued to present with hyperenhancement (arrow). (E) Pathologic microscopy shows that the tumor cells are epithelioid-like and arranged in a multinodular manner (×100, HE stain). (F) Multiple small vessels are also found in some areas (×100, CD34 stain). (G) The IHC finding is positive for HMB45 (×200). (H) The Ki-67 index is approximately 7% (×200).

The indications of an early draining vein have been previously suggested providing important diagnostic value for angiomyolipoma (22). Here, owing to draining of the draining vein into the hepatic vein, the early detection of the hepatic vein also imparts diagnostic value for epithelioid angiomyolipoma, reflecting the abundant blood supply within the tumor. Additionally, although the signs of an early draining vein have been reported in hepatic angiomyolipoma, we demonstrate its value in the imaging diagnosis of HEA. In contrast, an ill-defined draining vein is usually displayed in HCC lesions with a diameter greater than 12 cm (19). Compared with the large diameter of HCC, the diameters of the lesions of all HEA patients in our study were relatively small. Additionally, within our study, the draining vein was visible during the arterial phase in HEA with early indications of the hepatic vein. The inability to provide early detection of the hepatic veins in the HCC group in this study may be related to two causes. First, draining veins appear in HCCs larger than 12 cm in diameter; however, these lesions may be in an advanced stage that is not suitable for surgical treatment. For that reason, those patients were not included in our study. Second, due to the low incidence of HEA, we included relatively few cases of HCC and HEA in our study, which might have a certain effect on the observation of imaging features.

In contrast to previous reports, we did not focus on the early detection of the portal vein but rather focused on the drainage veins and hepatic veins. During the late arterial phase, the detection of the portal vein might be due to the return of mesenteric venous blood with a contrast agent to the portal vein rather than the return of the HEA drainage veins to the portal vein. Unlike the early detection of the portal vein, the hepatic vein is usually not displayed in the late arterial phase. Thus, the diagnostic specificity of the early detection of the hepatic vein during the arterial phase is relatively high. In addition, the early display of hepatic veins occurs only in one hepatic vein, while hepatic veins are usually displayed simultaneously under other conditions. Although the early display of the hepatic vein is not sensitive enough for the diagnosis of HEA, we demonstrate that it can still serve as an important diagnostic clue, especially in the case of failed identification between HEA and HCC by an enhancement pattern. Due to the relatively small number of HEA case reports, the diagnostic efficacy of the early display of the hepatic vein should also be further studied with a multicenter joint trial.

Another interesting finding is that the difference in intratumoral vessels during the arterial phase revealed by contrast-enhanced CT between both groups was nonsignificant, but the intratumoral vessels during the nonarterial phase could be valuable in the diagnosis of HEA. Unlike our findings, a comparative MRI study on hepatic angiomyolipoma and HCC found that intratumoral vessels could be more easily observed in hepatic angiomyolipoma than in HCC, and the occurrence rate of HEA was higher, reaching up to 88.9% (19). However, another observational study of HEA (5 cases) indicated that none of the HEA involved intratumoral vessels on contrast-enhanced MRI (22). Although the numbers of cases in these two studies were relatively low, these studies demonstrated a relatively large difference in the component ratios of vessels in HEA. In our study, the intratumoral vessels during the nonarterial phase on contrast-enhanced CT might be much more significant in the diagnosis of HEA. In our opinion, the intratumoral vessels of HEA were clearly defined during the nonarterial phase because the contrast agent remained for a long time after entering the thick-walled vessels.

In our study, half of the HEA cases showed a washout enhancement pattern similar to that of HCC, followed by prolonged enhancement (40%), whereas only a small number of HEA cases (8%) showed a fade pattern. Among these features, prolonged enhancement may be a valuable imaging characteristic of HEA since HEA was confirmed with rich sinusoid-like lacunae and vascular networks. Similarly, in a group of HEA cases in another study, prolonged enhancement occurred in more than half of the cases (6/9) with contrast-enhanced MRI (19). In contrast, prolonged enhancement of hepatic angiomyolipoma occurred in only one case in another study (23). The differences in these observations may be due to the relatively small sample of cases. When HEA exhibits prolonged enhancement, it can be differentiated from the washout enhancement pattern of typical HCC in contrast-enhanced CT. However, the performance of HCC may not be typical and have features such as prolonged enhancement and a fade pattern. Studies have confirmed that these atypical enhancement patterns of HCC are related to the diameter and differentiation of HCC (24). Small-diameter and well-differentiated HCCs harbor a relatively higher proportion of non-washout enhancement patterns (24). Currently, differentiating between HEA and HCC depending on the enhancement pattern is difficult, whereas other features, such as drainage veins and intralesional vascular enhancement, may play an important role. In addition, contrast-enhanced MRI examination should be performed as HCC harbors a higher proportion of typical washout enhancement patterns

on contrast-enhanced MRI than on contrast-enhanced CT (25). Additionally, as shown in previous studies, HEA can exhibit a washout enhancement pattern (19,22). When HEA exhibits a washout enhancement pattern, it is easy to misdiagnose as HCC. Other imaging features (such as the lack of intratumoral necrosis and enhanced vessels within lesions) and clinical characteristics (prevalence in females, no hepatitis B virus infection in the majority of cases or elevated AFP, etc.) of epithelioid angiomyolipoma are helpful for differential diagnosis. Finally, a small proportion of HEAs exhibit a fade pattern. Although this method of enhancement is not typical, a similar proportion of HCCs exhibit this enhancement model, creating a lack of specificity of enhancement patterns between these two groups.

Although the presence of a pseudocapsule was not significantly different between HEA and HCC in our study, the pseudocapsule warrants further investigation. Pathological findings confirm that HEA lacks a true capsule and that large-size HEA can have pseudocapsules due to compression by the surrounding liver tissue (10). However, the proportion of pseudocapsules observed in different HEA imaging studies was significantly different. For instance, in a study of six HEA cases, pseudocapsules occurred in only one HEA on contrast-enhanced CT and MRI (10). In another study concerning hepatic angiomyolipoma, pseudocapsules did not appear in all 18 cases (26). Consistent with these studies, the proportion of pseudocapsules was low in our study (only 12%). However, in a group of 11 cases of hepatic angiomyolipoma (including five cases of HEA), pseudocapsules were observed in all five cases of HEA and in most nonepithelial (4/6) cases (20). We propose that different imaging methods might affect the observation of pseudocapsules. In clinical practice, pseudocapsules are often helpful diagnostic features in HCC. However, in our study, the proportion of pseudocapsules was lower in contrast-enhanced CT. This finding might be due to relatively less fibrous tissue in noncirrhotic liver tissues surrounding HCC.

Notably, our study has several limitations. First, although the number of cases in our study is acceptable compared with the numbers in previous studies, it is still small. Second, as this study was retrospective, data consistency may be affected by the collection of case images over a long period due to various unmanageable factors, such as the replacement of contrast agent and optimization of imaging systems. Third, the evaluation of imaging data in this study was completed independently by two experienced radiologists from our institution. However, some imaging features lack unified and unambiguous definitions. Thus, with an increased understanding of HEA, the relevant imaging signs must be further defined, and a consensus must be reached.

Overall, in our study, HEA was more prevalent among females, with an average age near 50 years old. HEA usually manifests as a necrosis-free, fat-deficient mass with an abundant blood supply on CT. The early display of the hepatic vein during the arterial phase, intratumoral blood vessels during the nonarterial phase, and prolonged enhancement patterns are clues to the differential diagnosis of HEA from HCC in noncirrhotic livers.

Acknowledgements

None.

Footnote

Conflicts of Interest: The authors have no conflicts of interest to declare.

Ethical Statement: This retrospective study was approved by the Ethics Committee of the First Affiliated Hospital, College of Medicine, Zhejiang University (No. 201749).

References

1. Ishak KG. Mesenchymal tumors of the liver. In: Okuda K, Peters RL. editors. Hepatocellular carcinoma. New York: John Wiley, 1976:247-304.
2. Kudo M, Okuno T, Tomita S, Kajiwara T, Shirane H, Usuki N, Todo A. Hepatic angiomyolipoma preoperatively diagnosed by imaging. J Gastroenterol Hepatol 1993;8:483-8.
3. Kawarada Y, Mizumoto R. Angiomyolipoma of the liver. Am J Gastroenterol 1983;78:434-9.
4. Tsui WM, Colombari R, Portmann BC, Bonetti F, Thung SN, Ferrell LD, Nakanuma Y, Snover DC, Bioulac-Sage P, Dhillon AP. Hepatic angiomyolipoma: a clinicopathologic study of 30 cases and delineation of unusual morphologic variants. Am J Surg Pathol 1999;23:34-48.
5. Lu HC, Chau GY, Su CW. Clinical challenges and images in GI. Diagnosis: Hepatic angiomyolipoma mimicking hepatocellular carcinoma. Gastroenterology 2009;136:1169, 1464.
6. Yamasaki S, Tanaka S, Fujii H, Matsumoto T, Okuda C, Watanabe G, Suda K. Monotypic epithelioid

angiomyolipoma of the liver. Histopathology 2000;36:451-6.
7. Flemming P, Lehmann U, Becker T, Klempnauer J, Kreipe H. Common and epithelioid variants of hepatic angiomyolipoma exhibit clonal growth and share a distinctive immunophenotype. Hepatology 2000;32:213-7.
8. Liu J, Zhang CW, Hong DF, Tao R, Chen Y, Shang MJ, Zhang YH. Primary hepatic epithelioid angiomyolipoma: A malignant potential tumor which should be recognized. World J Gastroenterol 2016;22:4908-17.
9. Mete O, van der Kwast TH. Epithelioid angiomyolipoma: a morphologically distinct variant that mimics a variety of intra-abdominal neoplasms. Arch Pathol Lab Med 2011;135:665-70.
10. Yang B, Chen WH, Li QY, Xiang JJ, Xu RJ. Hepatic angiomyolipoma: dynamic computed tomography features and clinical correlation. World J Gastroenterol 2009;15:3417-20.
11. Ji JS, Lu CY, Wang ZF, Xu M, Song JJ. Epithelioid angiomyolipoma of the liver: CT and MRI features. Abdom Imaging 2013;38:309-14.
12. Tan Y, Xie X, Lin Y, Huang T, Huang G. Hepatic epithelioid angiomyolipoma: clinical features and imaging findings of contrast-enhanced ultrasound and CT. Clin Radiol 2017;72:339.e1-339.e6.
13. Available online: http://www.acr.org/Quality-Safety/Resources/LIRADS
14. Ferlay J, Shin HR, Bray F, Forman D, Mathers C, Parkin DM. Estimates of worldwide burden of cancer in 2008: GLOBOCAN 2008. Int J Cancer 2010;127:2893-917.
15. Yuen MF, Ahn SH, Chen DS, Chen PJ, Dusheiko GM, Hou JL, Maddrey WC, Mizokami M, Seto WK, Zoulim F, Lai CL. Chronic Hepatitis B Virus Infection: Disease Revisit and Management Recommendations. J Clin Gastroenterol 2016;50:286-94.
16. El-Serag HB. Epidemiology of viral hepatitis and hepatocellular carcinoma. Gastroenterology 2012;142:1264-73.e1.
17. Chuang SC, Lee YC, Hashibe M, Dai M, Zheng T, Boffetta P. Interaction between cigarette smoking and hepatitis B and C virus infection on the risk of liver cancer: a meta-analysis. Cancer Epidemiol Biomarkers Prev 2010;19:1261-8.
18. Aydin H, Magi-Galluzzi C, Lane BR, Sercia L, Lopez JI, Rini BI, Zhou M. Renal angiomyolipoma: clinicopathologic study of 194 cases with emphasis on the epithelioid histology and tuberous sclerosis association. Am J Surg Pathol 2009;33:289-97.
19. Wang SY, Kuai XP, Meng XX, Jia NY, Dong H. Comparison of MRI features for the differentiation of hepatic angiomyolipoma from fat-containing hepatocellular carcinoma. Abdom Imaging 2014;39:323-33.
20. Chen LS, Zhu ZQ, Wang ZT, Li J, Liang LF, Jin JY, Wang ZQ. Chemical shift magnetic resonance imaging for distinguishing minimal-fat renal angiomyolipoma from renal cell carcinoma: a meta-analysis. Eur Radiol 2018;28:1854-61.
21. Yoon JH, Lee JM, Suh KS, Lee KW, Yi NJ, Lee KB, Han JK, Choi BI. Combined Use of MR Fat Quantification and MR Elastography in Living Liver Donors: Can It Reduce the Need for Preoperative Liver Biopsy? Radiology 2015;276:453-64.
22. Zhao Y, Ouyang H, Wang X, Ye F, Liang J. MRI manifestations of liver epithelioid and nonepithelioid angiomyolipoma. J Magn Reson Imaging 2014;39:1502-8.
23. Jeon TY, Kim SH, Lim HK, Lee WJ. Assessment of triple-phase CT findings for the differentiation of fat-deficient hepatic angiomyolipoma from hepatocellular carcinoma in non-cirrhotic liver. Eur J Radiol 2010;73:601-6.
24. Park VY, Choi JY, Chung YE, Kim H, Park MS, Lim JS, Kim KW, Kim MJ. Dynamic enhancement pattern of HCC smaller than 3 cm in diameter on gadoxetic acid-enhanced MRI: comparison with multiphasic MDCT. Liver Int 2014;34:1593-602.
25. Lee YJ, Lee JM, Lee JS, Lee HY, Park BH, Kim YH, Han JK, Choi BI. Hepatocellular carcinoma: diagnostic performance of multidetector CT and MR imaging-a systematic review and meta-analysis. Radiology 2015;275:97-109.
26. Cai PQ, Wu YP, Xie CM, Zhang WD, Han R, Wu PH. Hepatic angiomyolipoma: CT and MR imaging findings with clinical-pathologic comparison. Abdom Imaging 2013;38:482-9.

Cite this article as: Liu W, Liang W. CT features of hepatic epithelioid angiomyolipoma: differentiation from hepatocellular carcinoma in patients with noncirrhotic livers. Quant Imaging Med Surg 2018;8(6):597-608. doi: 10.21037/qims.2018.07.01

